

OVER THREE YEARS OF ROVER LOCALIZATION AND TOPOGRAPHIC MAPPING FOR MER 2003

MISSION. R. Li¹, K. Di¹, B. Wu¹, W. Chen¹, M.W. Maimone², L.H. Matthies², L. Richter³, R. Kirk⁴, R. Sullivan⁵, L. Crumpler⁶, T. Parker², D. Des Marais⁷, R. Arvidson⁸, M.H. Sims⁷, S. Squyres⁵, and the Athena Science Team, ¹Mapping and GIS Laboratory, CEEGS, The Ohio State University, 470 Hitchcock Hall, 2070 Neil Ave., Columbus, OH 43210-1275, li.282@osu.edu, ²Jet Propulsion Laboratory, California Institute of Technology, Pasadena, CA, ³DLR Institut für Raumsimulation, Köln, Germany, ⁴U.S. Geological Survey, Flagstaff, AZ, ⁵Center for Radio-physics and Space Research, Cornell University, Ithaca, NY, ⁶New Mexico Museum of Natural History and Science, Albuquerque, NM, ⁷Ames Research Center, Moffett Field, CA, ⁸Washington University, St. Louis, MO.

Introduction: The two 2003 Mars Exploration Rover (MER) mission rovers, Spirit and Opportunity, have been exploring the Martian surface for over three years. As of April 10, 2007 (Sol 1162 for Spirit; Sol 1141 for Opportunity), Spirit has traveled 6.3 km while Opportunity has traveled 10.0 km (actual distances traveled, not odometry measures). Topographic maps, rover traverse maps, and updated rover locations for the rovers [1, 2, 3] have been produced and distributed to the science and engineering team members through a WebGIS, for science analysis, long term planning and operations [4, 5, 6, 7]. In this abstract, we outline the rover localization and mapping results and products produced over the past three years of operations.

Rover Localization: On-board rover localization is performed using wheel odometry, IMU, and a Sun positioning technique using Pancam imagery. A visual odometry technique is applied in order to correct errors caused by wheel slippage within a site, particularly on difficult terrain or when approaching a target. In order to achieve high accuracy over long distances, bundle adjustment (BA) of an image network formed by Pancam and/or Navcam images is carried out on Earth.

Navcam/Pancam panoramic images, and, occasionally, forward- and backward-looking Navcam/Pancam middle-point survey images. Figure 1 shows the Spirit bundle-adjusted traverse map as of Sol 1153. Overall, after BA, 2D accuracy is sub-pixel to 1.5 pixels and 3D accuracy is at a centimeter to sub-meter level based on consistency check of the BA results [2, 3].

From Sol 154 to Sol 732 of Spirit rover, we performed a local comparison of rover traverses in the Husband Hill area, where Spirit experienced significant wheel slippage climbing the hill (Figure 2). In this area, the locally accumulated relative difference between the telemetry-derived traverse and the bundle-adjusted traverse was 0.4 % to 10.5 %, with a maximum of 10.5 % (56.6 m over 540.6 m) on Sol 337. The maximum absolute difference was 82.06 m, found on Sol 648. This demonstrates that the BA was able to correct significant localization errors. We also found that the up-slope and down-slope slippages were cancelled out to a significant extent. Currently we are analyzing this slippage event considering local terrain and surface properties.

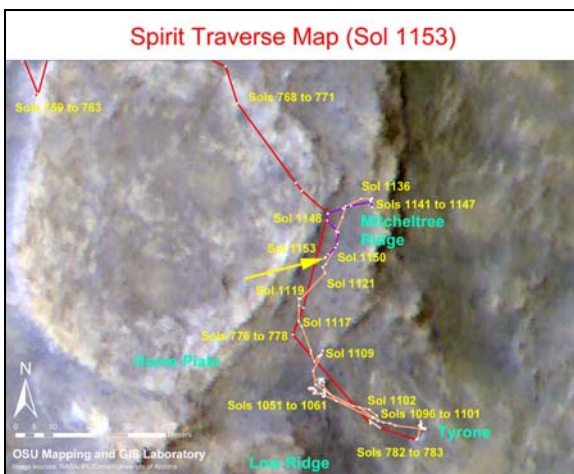


Figure 1. Spirit traverse map (Sol 1153).

At the Gusev Crater landing site, localization of the Spirit rover has been performed sol by sol based on incremental bundle adjustment using full or partial

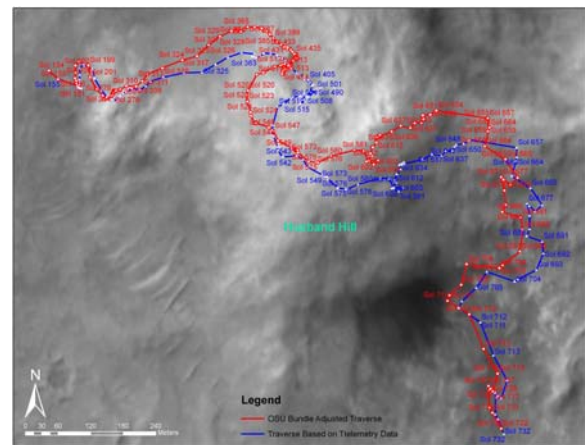


Figure 2. Spirit rover traverses from telemetry (blue) and BA (Red) from Sol 154 to Sol 732.

At the Meridiani Planum landing site, we conducted a BA within Eagle Crater (up to Sol 62) that was able to correct a localization error (mainly caused by wheel slippage) as large as 21 percent. After leaving Eagle Crater, BA-based rover localization was

impossible due to insufficient localization image data. However, wherever we observed large features (craters such as the Fram, Endurance, Argo, Jason, Naturaliste, Vostok and, most recently, Victoria craters) we were able to generate orthophotos of these features and compare them with the MOC NA or HiRISE base map. The results were then used to adjust the rover traverse. In particular, the rover itself and part of the rover track can be seen in the HiRISE image acquired on October 3, 2006. This helped to improve the consistency between the rover traverse and the HiRISE base map. Figure 3 shows the Opportunity traverse map as of Sol 1132 along Victoria crater rim. Though not optimal, this adjustment strategy enabled us to provide the 2D Opportunity traverse in a timely manner.



Figure 3. Opportunity traverse map (Sol 1132).

Topographic Mapping: Various kinds of topographic products have been generated to meet the needs of the mission scientists and engineers. These include traverse maps, detailed 3D terrain models, slope maps, orthophotos, solar energy maps, and drive metrics. So far, we have generated topographic products including over 120 orthophotos and DTMs (digital terrain models), and six 3D crater models as well as periodic traverse maps and vertical profiles. Many of these topographic products were automatically generated from single-site panoramic stereo images. Figure 4 shows an orthophoto automatically generated from the Navcam panorama taken by Spirit rover on Sols 799-801. Some of these products were detailed 3D models of major features generated from multi-site panoramic stereo hard baseline and wide baseline images. These include large DTMs of the Husband Hill summit area, south inner basin, McCool Hill, and Home Plate at Gusev Crater, as well as Endurance and Victoria craters at Meridiani Planum.

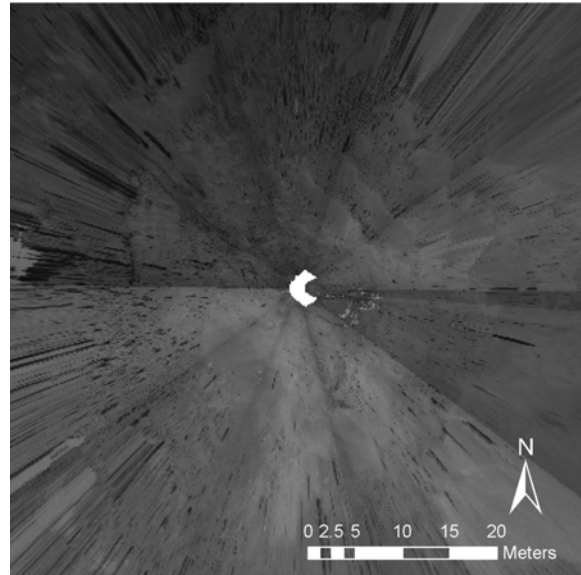


Figure 4. Orthophoto generated from Navcam images taken by Spirit on Sols 799-801 (60×60m, 5cm/pixel).

We also produced special topographic products, such as north-facing slope maps and solar energy maps (with collaboration of the USGS). Figure 5 shows the central part (690×640 meters) of the DTM in the Husband Hill area on top of a MOC NA base map along with contours derived from a USGS DTM (based on orbital data). During the past Martian winter, these maps were very helpful for choosing areas where the Spirit rover could have sufficient solar energy.

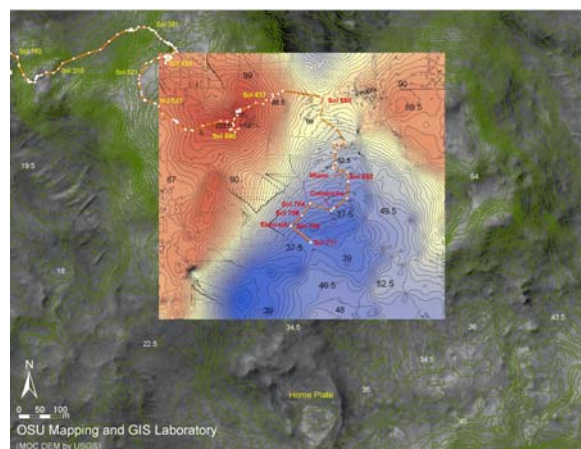


Figure 5. Topographic map of Husband Hill summit, inner basin, and Home Plate.

Since Sol 951, Opportunity has been exploring the north rim of Victoria Crater, studying the layers in crater walls, topography of inside slopes, outcrops and sand dune features, and so forth. Several bays along the rim are examined as candidates for the rover to

safely ingress and exit the crater. Topographic products are essential for this purpose.

We mapped Duck Bay using hard (rover) baseline Pancam images from Sol 953. Figure 6 shows the DTM and derived contour map (1-m intervals). Figure 7 shows a slope map derived from the DTM. Figure 8 shows the 3D surface of Duck Bay. The Pancam orthophoto was projected onto the 3D surface to give information on the surface material. This is shown in Figure 9.

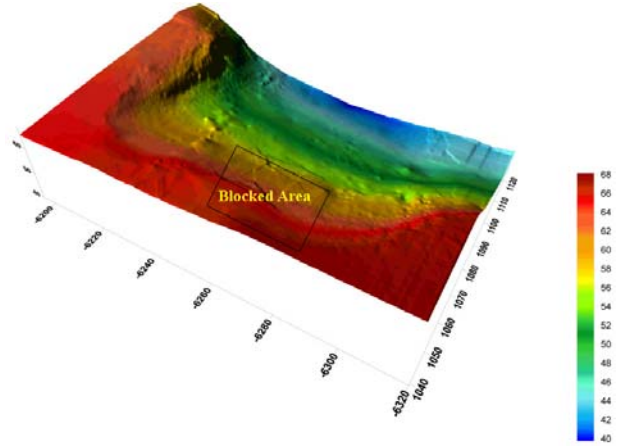


Figure 8. 3D surface of Duck Bay.

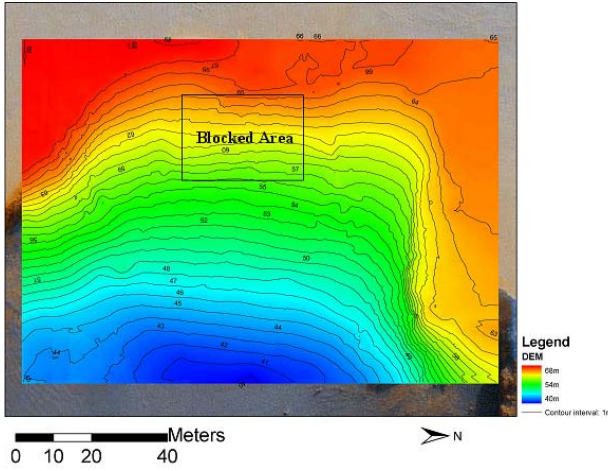


Figure 6. DTM and contour map of Duck Bay.

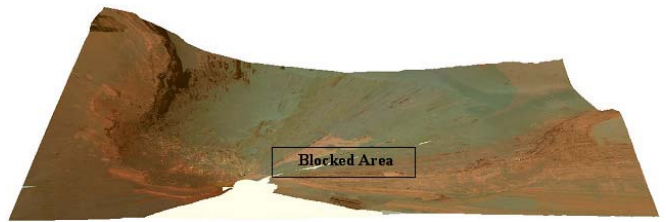


Figure 9. Color orthophoto draped on the 3D surface of Duck Bay.

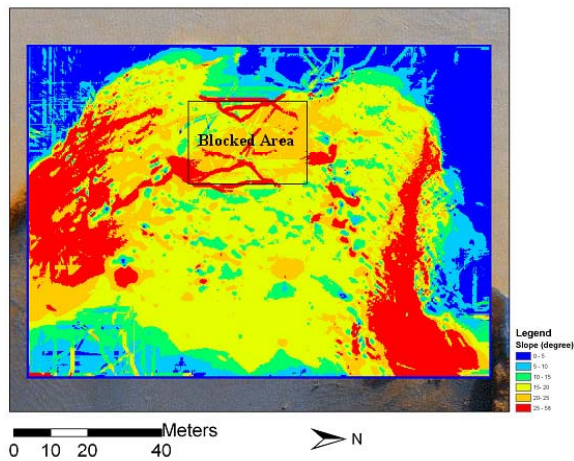


Figure 7. Duck Bay slope map.

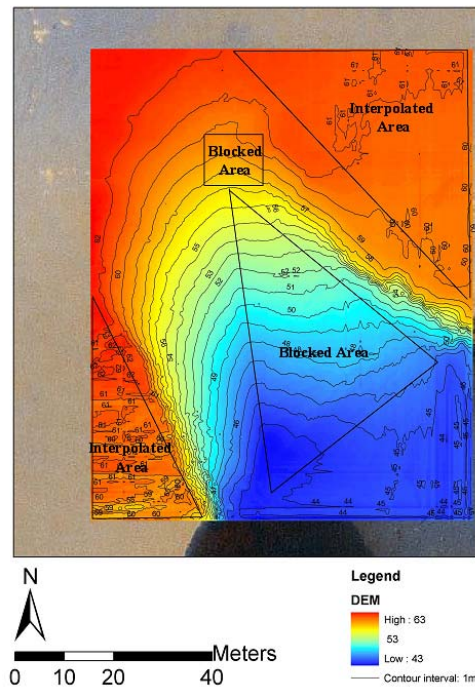


Figure 10. DTM and contour map of Bottomless Bay.

We mapped Bottomless Bay using multi-site images, including wide baseline (2.5 m) Pancam images from Sols 1034 and 1036, wide baseline (5.2 m) Pancam images from Sols 1019 and 1021, and hard baseline Pancam images from Sols 1021 and 1029. An integrated DTM was generated using 3D points from all these positions. Figure 10 shows the DTM and derived contour map (1-m intervals). Figure 11 shows a slope map derived from the DTM. Figure 12 is a 3D view of the DTM. Figure 13 shows a 3D view of the Pancam orthophoto draped on the DTM.

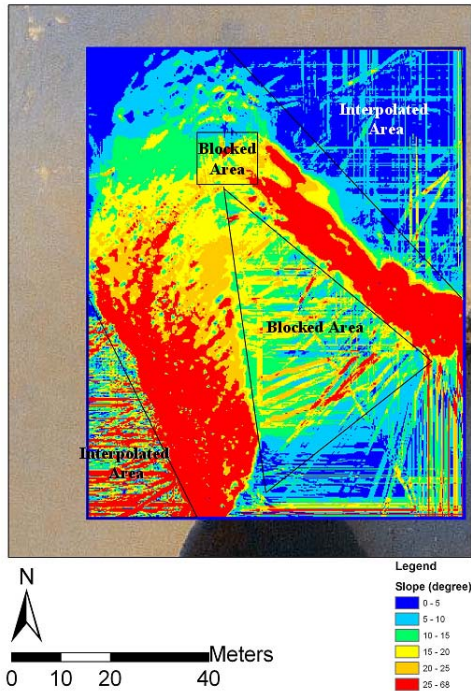


Figure 11. Bottomless Bay slope map.

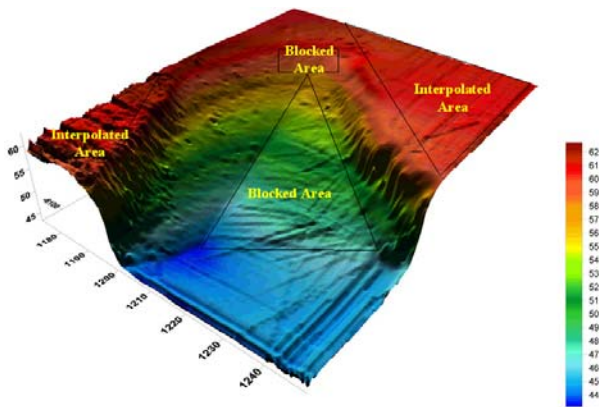


Figure 12. 3D surface of Bottomless Bay.

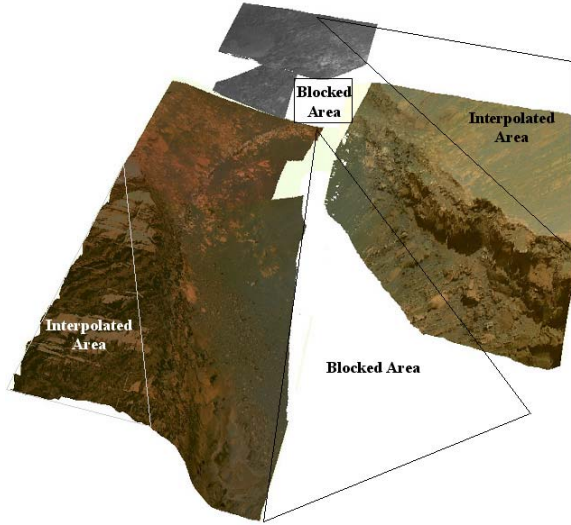


Figure 13. Color orthophoto draped on the 3D surface of Bottomless Bay.

References: [1] Li, R. et al. (2005) *PE&RS*, 71(10), 1129-1142. [2] Li, R. et al. (2006) *JGR*, 111(E2), E02S06. [3] Li, R. et al. (2007) *JGR*, 112(E2), E02S90. [4] Squyres, S.W. (2004) *Science*, 305(5685), 794-799. [5] Squyres, S.W. (2004) *Science*, 306(5702), 1698-1703. [6] Arvidson, R. E. et al. (2004) *Science*, 305(5685), 821-824. [7] Arvidson, R.E. (2004) *Science*, 306(5702), 1730-1733.

Acknowledgements: We would like to thank Pancam team, HiRISE team and MOC Team for their images used in the work.